

Semilocal Density Functional Theory with correct surface asymptotics

Lucian A. Constantin,¹ Eduardo Fabiano,^{2,1} J. M. Pitarke,^{3,4} and Fabio Della Sala^{2,1}

¹Center for Biomolecular Nanotechnologies @UNILE,

Istituto Italiano di Tecnologia, Via Barsanti, I-73010 Arnesano, Italy

²Istituto Nanoscienze-CNR, Euromediterranean Center for Nanomaterial

Modelling and Technology (ECMT), via Arnesano 73100, Lecce

³CIC nanoGUNE, Tolosa Hiribidea 76, E-20018 Donostia, Basque Country

⁴Materia Kondentsatuaren Fisika Saila, DIPC, and Centro Física Materiales CSIC-UPV/EHU,

644 Posta kutxatila, E-48080 Bilbo, Basque Country

(Dated: November 24, 2020)

Semilocal Density Functional Theory is the most used computational method for electronic structure calculations in theoretical solid-state physics and quantum chemistry of large systems, providing good accuracy with a very attractive computational cost. Nevertheless, because of the non-locality of the exchange-correlation hole outside a metal surface, it was always considered inappropriate to describe the correct surface asymptotics. Here, we derive, within the semilocal Density Functional Theory formalism, an exact condition for the image-like surface asymptotics of both the exchange-correlation energy per particle and potential. We show that this condition can be easily incorporated into a practical computational tool, at the simple meta-generalized-gradient approximation level of theory. Using this tool, we also show that the Airy-gas model exhibits asymptotic properties that are closely related to the ones at metal surfaces. This result highlights the relevance of the linear effective potential model to the metal surface asymptotics.

PACS numbers: 71.10.Ca, 71.15.Mb, 71.45.Gm

I. INTRODUCTION

The exact form of the potential felt by an electron leaving from or approaching a metal surface is of great importance for a variety of physical phenomena, including the interpretation of image states¹, modeling quantum-transport², low-energy electron diffraction (LEED)³, scanning tunneling microscopy^{4,5}, and inverse or two-photon photoemission spectroscopy^{6,7}. The asymptotic form of this image potential is $-1/(4(z-z_0))$, with z being the distance from the surface, and z_0 representing the position of the so-called image plane⁸, and should be reproduced by any computational method aiming at an accurate description of the surface physics.

Within Kohn-Sham (KS) density-functional theory (DFT)^{9,10}, which is the most used computational method for electronic structure calculations in theoretical solid-state physics, the shape of the image potential is dictated by the properties of the effective Kohn-Sham (KS) potential. This depends on the employed approximation for the exchange-correlation (XC) functional $E_{xc}[\rho]$, which gives the XC potential via the relation

$$v_{xc}(\mathbf{r}) = \frac{\delta E_{xc}[\rho]}{\delta \rho(\mathbf{r})}, \quad (1)$$

where ρ is the electron density. It has been shown that the exact v_{xc} asymptotically approaches the image potential^{8,11-14}, despite a different result has been obtained within the plasmon-pole approximation¹⁵.

The popular local density approximation (LDA)¹⁰ and the generalized-gradient approximation (GGA), however, fail in this task¹⁶ showing either a too fast decay (e.g. exponential), or an inaccurate description of the surface

energetics (as for the Becke exchange¹⁷). Ad-hoc modifications of the LDA XC potential^{18,19} have then been proposed to improve the asymptotic behavior of the XC potential, but such methods are not functional derivatives of any energy functional. Alternatively, non-local methods outside the KS framework^{11,13,14,20-22} are employed.

An accurate KS-DFT method with the correct surface asymptotics would be desirable for many reasons, including the local nature and the computational efficiency. However, a good functional shall yield not only the correct asymptotic XC potential, but also accurate energies. Thus, it is necessary to be defined by a realistic energy per particle $\epsilon_{xc}(\mathbf{r})$. The latter is not a uniquely defined physical quantity, but an exact reference for it is the the conventional energy per particle, which is associated with the interaction of an electron at \mathbf{r} with the coupling-constant-averaged charge of its XC hole²³⁻²⁵. The exact (conventional) $\epsilon_{xc}(\mathbf{r})$ at metal surfaces decays as $-1/(4(z-z_0))$, i.e. as the image potential^{11,26}.

We recall that the exact exchange energy per particle decreases as $\epsilon_x(z \rightarrow \infty) \rightarrow -A(\beta)/z$ where $A(\beta) = (\pi + 2\beta \ln(\beta))/(2\pi(1 + \beta^2))$, $\beta = \sqrt{\epsilon_F/W}$, $\epsilon_F = k_F^2/2$ being the Fermi energy (and k_F the Fermi wavevector), and W the work function^{27,28}. On the other hand, the exact exchange potential behaves as $v_x(z \rightarrow \infty) \rightarrow \ln(\beta k_F z)/(2\pi\beta z)$ ²⁹. Note that these behaviors are related to semi-infinite surfaces; for finite jellium slabs we have that, as in molecules, $\epsilon_x(z \rightarrow \infty) = -1/(2z)$ ²⁷ and $v_x(z \rightarrow \infty) = -1/(z)$ ³⁰⁻³⁴.

The simultaneous description of surface asymptotic and energy properties is anyway an ambitious objective, which is in fact not achievable at the GGA level³⁵⁻³⁸. In

this article, we show that the issue can be instead solved at the meta-GGA level of theory, employing an exact condition which yields the correct image-like asymptotic behavior of both ϵ_{xc} and v_{xc} at metal surfaces. This condition can be easily implemented in any meta-GGA functional, keeping its original accuracy for ground-state properties not related to surface asymptotics. Hence, an accurate KS-DFT method with correct metal-surface asymptotic can be obtained for application in many surface science problems.

II. EXACT CONDITION FOR ASYMPTOTIC PROPERTIES

To start, we consider the simplest (and most used) model for a metal surface: the semi-infinite jellium surface. This model system is very important in surface science and solid-state physics, containing the physics of simple metal surfaces^{8,39,40}.

The KS single-particle orbitals have the form

$$\Psi_{k_z, \mathbf{k}_{||}}(\mathbf{r}) = \frac{1}{\sqrt{S}\sqrt{L}} e^{i\mathbf{k}_{||}\mathbf{r}_{||}} \phi_{k_z}(z), \quad (2)$$

where $\mathbf{k}_{||}$ and $\mathbf{r}_{||}$ are the two-dimensional wave-vector and position vector in the plane xy of the surface, k_z and z are the corresponding components in the direction perpendicular to the surface, S and L are the normalization area and length, and $\phi_{k_z}(z)$ are the eigenfunctions of a one-dimensional KS Hamiltonian (for details see Appendix A).

In the vacuum region, far away from the surface ($z \rightarrow \infty$), the single-particle orbitals $\phi_{k_z}(z)$ behave as²⁷:

$$\phi_{k_z}(z \rightarrow \infty) \rightarrow \phi_{k_F}(z \rightarrow \infty) e^{-\beta z(k_F - k_z)}, \quad (3)$$

where

$$\phi_{k_F}(z \rightarrow \infty) \sim e^{-z\sqrt{2W}} (2z\sqrt{2W})^{\alpha_{KS}/\sqrt{2W}}, \quad (4)$$

$\alpha_{KS} > 0$.

Now, we consider a meta-GGA XC energy per particle of the form

$$\epsilon_{xc}^{MGGA} = \epsilon_x^{LDA} \frac{1}{\eta} \frac{8\pi}{3\sqrt{5}} \frac{\sqrt{\alpha}}{\sqrt{\ln(\alpha)}}, \quad (5)$$

where η is a parameter to be fixed later, $\alpha(\mathbf{r}) = [\tau(\mathbf{r}) - \tau^W(\mathbf{r})]/\tau^{TF}(\mathbf{r})$ is the well-known meta-GGA ingredient that measures the non-locality of the kinetic-energy density³⁸, with τ , τ^W , and τ^{TF} being the positive-defined exact KS, von Weizsäcker, and Thomas-Fermi kinetic-energy densities, respectively. We recall that $1/[1 + \alpha(\mathbf{r})^2]$ is the electron localization function, often used in the characterization of chemical bonds⁴¹. Eq. (5) yields the following asymptotic behaviors (see the Appendix B for details):

$$\epsilon_{xc}^{MGGA}(z \rightarrow \infty) \rightarrow -\frac{1}{\eta} \frac{1}{z} + \mathcal{O}(z^{-2}), \quad (6)$$

$$v_{xc}^{MGGA}(z \rightarrow \infty) \rightarrow -\frac{3}{2\eta} \frac{1}{z} + \mathcal{O}(z^{-2}). \quad (7)$$

Here, the KS potential has been obtained in the generalized KS framework using the formula⁴²

$$v_{xc}(\mathbf{r})\Psi_i(\mathbf{r}) = \left[\frac{\partial(\rho\epsilon_{xc})}{\partial\rho} - \nabla \frac{\partial(\rho\epsilon_{xc})}{\partial\nabla\rho} \right] \Psi_i - \frac{1}{2} \nabla \left(\frac{\partial(\rho\epsilon_{xc})}{\partial\tau} \right) \nabla \Psi_i - \frac{1}{2} \frac{\partial(\rho\epsilon_{xc})}{\partial\tau} \nabla^2 \Psi_i. \quad (8)$$

Equations. (6) and (7) show that, in contrast to previously developed XC functionals, both v_{xc} and ϵ_{xc} are proportional to the exact ones: if $\eta = \eta_1 = 4$ ($\eta = \eta_2 = 6$) then the exact energy-density (potential) is obtained. Unfortunately, $\eta_1 \neq \eta_2$. Nevertheless, for both values Eq. (5) yields an asymptotic behavior qualitatively and quantitatively significantly beyond the current state-of-the-art. We also remark that Eq. (5) is solely based on the properties of the reduced kinetic ingredient α . However, at the meta-GGA level of theory, other ingredients are also available (e.g. the gradient and the Laplacian of the density) so that the exact asymptotic description of both ϵ_{xc} and v_{xc} might be achieved.

III. PRACTICAL COMPUTATIONAL TOOL

As a first practical example, we consider the case $\eta = \eta_1$ and incorporate the condition of Eq. (5) into the popular TPSS meta-GGA functional⁴³, using an approach similar to that of Ref. 44. The resulting XC functional will be termed surface-asymptotics (SA) TPSS. This functional is obtained by simply changing, in the TPSS exchange formula, the parameter κ (which determines the asymptotic behavior of the functional) from its original value of 0.804 to

$$\kappa = \frac{2\pi}{3\sqrt{5}} \frac{\sqrt{\alpha+1}}{\sqrt{a + \ln(\alpha+b)}}. \quad (9)$$

The correlation is left unchanged. (Note that the TPSS correlation decays exponentially, and thus our XC condition is incorporated in the TPSS exchange functional. This is a common procedure for semilocal functionals, which are based on a strong error cancellation between the exchange and correlation parts.) In Eq. (9), the parameters $a = 2.413$ and $b = 0.348$ have been fixed by imposing the constraints: $\kappa = 0.804$ for $\alpha = 1$ and $\alpha = 0$; whereas, when degenerate orbitals contribute to the tail of the density ($\alpha \rightarrow \infty$), $\kappa \rightarrow \frac{2\pi}{3\sqrt{5}} \frac{\sqrt{\alpha}}{\sqrt{\ln(\alpha)}}$ (i.e. Eq. (5)).

These conditions assure that (i) all the exact constraints satisfied by the original TPSS exchange functional are preserved and (ii) the new functional yields the correct image-like asymptotics. The SA-TPSS functional does not recover locally the Lieb-Oxford bound⁴⁴, as TPSS does, but it satisfies the global Lieb-Oxford bound for all known physical systems (e.g. for atoms, molecules, solids and surfaces $E_{xc}^{SA-TPSS} \approx E_{xc}^{TPSS}$). Moreover, it fulfills locally the simplified version of the Lewin-Lieb bound (see Eq. (22) of Ref.⁴⁵).

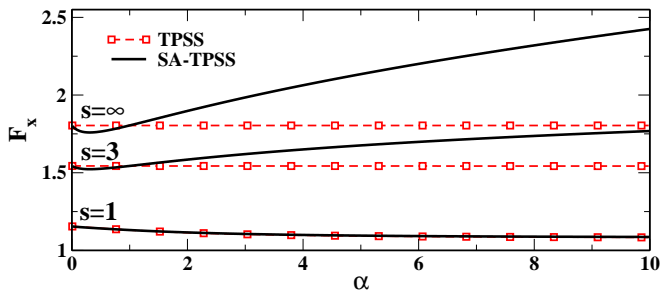


FIG. 1: TPSS and SA-TPSS exchange enhancement factors versus α , for three values of the reduced gradient s .

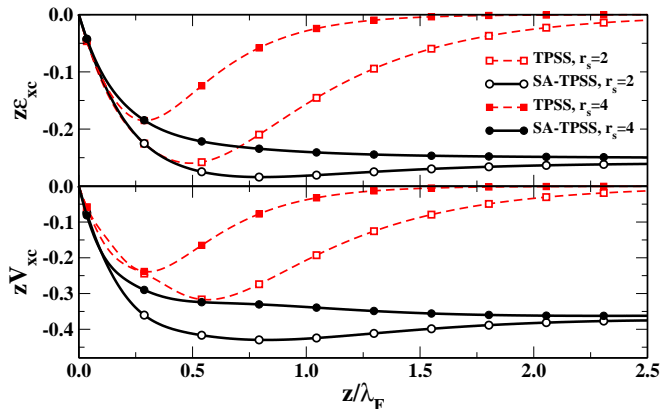


FIG. 2: $z\epsilon_{xc}(z)$ (upper panel) and $zv_{xc}(z)$ (lower panel) versus the reduced distance z/λ_F (λ_F is the Fermi wavelength), for a jellium surface with electron-density parameter $r_s = 2$ and $r_s = 4$. The surface is located at $z = 0$. Note that SA-TPSS gives $z\epsilon_{xc} = -1/4$ and $zv_{xc} = -3/8$ far outside the surface.

In Fig. 1, we show the TPSS and SA-TPSS exchange enhancement factors versus α for several values of the reduced gradient $s = |\nabla\rho|/(2(3\pi^2)^{1/3}\rho^{4/3})$. When s is small, TPSS and SA-TPSS coincide for all values of α . As s increases, TPSS and SA-TPSS start to differ, especially at large values of α , as expected.

In Fig. 2, fully self-consistent KS-LDA orbitals were used to obtain $z\epsilon_{xc}(z)$ (upper panel) and $zv_{xc}(z)$ (lower panel) as a function of the scaled distance z for jellium surfaces with the electron-density parameters $r_s = 2$ and $r_s = 4$. The TPSS functional yields a wrong (exponential) asymptotic behavior for both quantities. Instead, the SA-TPSS functional gives the following asymptotic behaviors: $\epsilon_{xc}(z) \rightarrow -0.25/z$ and $v_{xc}(z) \rightarrow -0.375/z$. Thus, Fig. 2 provides a numerical proof of the validity of Eq. (5), as well as a validation of the simple construction used to obtain the SA-TPSS functional.

In Tables I and II we report the TPSS and SA-TPSS results for surface energies and various molecular tests, respectively. By construction, whenever the surface asymptotics plays a negligible role (e.g., covalent interactions in molecules: W4, OMRE, IP13, MGBL19) both functionals yield very similar results. In the case of jellium surface energies and non-covalent interactions (DI6, HB6),

TABLE I: Jellium surface energies (in erg/cm²), as obtained by using the functionals TPSS and SA-TPSS for various values of the electron-density parameter r_s . Diffusion Monte Carlo (DMC) calculations⁴⁶ are given as a reference. The results of the popular LDA^{10,47} and PBE⁴⁸ functionals, are also shown for comparison.

r_s	TPSS	SA-TPSS	LDA	PBE	Ref.
2	3380	3368	3354	3265	3392 ± 50
3	772	767	764	741	768 ± 10
4	266	263	261	252	261 ± 8
6	55.5	54.5	53	52	53 ± ...

TABLE II: Mean absolute errors (in kcal/mol for energetical tests and in mÅ for the bond length test) of several molecular properties^{49,50}.

Test	TPSS	SA-TPSS	LDA	PBE
atomization energies (W4 test)	4.7	4.8	44.0	10.7
reaction energies (OMRE test)	8.0	7.9	21.0	6.7
ionization potentials (IP13 test)	3.1	3.1	4.9	3.0
bond lengths (MGBL19 test)	6.9	7.0	10.0	9.3
dipole interactions (DI6 test)	0.6	0.4	2.7	0.4
hydrogen bonds (HB6 test)	0.6	0.4	4.5	0.4

however, SA-TPSS improves over the standard TPSS.

Finally, we have to stress that the SA-TPSS meta-GGA gives only the correct asymptotic decay of the XC energy per particle and potential at metal surfaces, but it can not provide the exact behavior for the exchange and correlation components, separately. This is a difficult task, that in our opinion, a simple semilocal functional can not obey.

IV. AIRY GAS ASYMPTOTIC PROPERTIES

As an additional example of the use of Eq. (5) and of the SA-TPSS functional, we consider the Airy gas^{51,52}, which is the simplest possible model for an edge electron gas (for details see Appendix A). This model system plays an important role in DFT⁵²⁻⁵⁴, as it incorporates the correct physics of a semi-infinite metal surface and is simple enough to allow for analytical calculations. To our knowledge, the exact asymptotic behavior of the XC energy per particle and of KS XC potential of the Airy gas are unknown. Nevertheless, we can use the SA-TPSS functional to obtain some information about them.

The Airy-gas electron density and positive-defined kinetic-energy density are^{51-53,55}

$$\rho(z) = \frac{1}{3\pi} [z^2 \text{Ai}^2(z) - z \text{Ai}'^2(z) - \text{Ai}(z) \text{Ai}'(z)/2], (10)$$

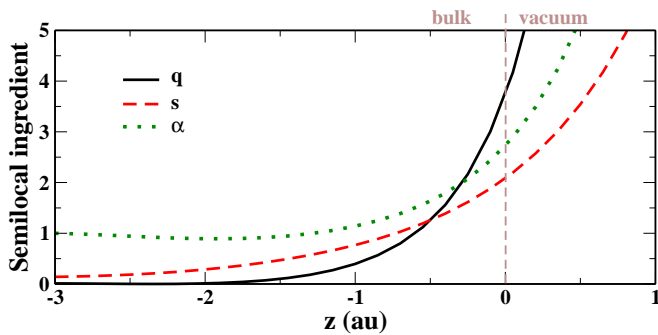


FIG. 3: The Airy-gas semilocal ingredients (s , q , and α), as a function of the scaled distance z . The Airy bulk is at $z \leq 0$. The exponential decay of the electron density occurs at $z \geq 0$.

$$\tau = -\frac{3}{10}z\rho(z) + \frac{1}{5}\rho''(z), \quad (11)$$

where z is the scaled distance and $\text{Ai}(z)$ is the Airy function. In Fig. 3, we show the Airy-gas semilocal ingredient s , the reduced Laplacian $q = \nabla^2\rho/[4(3\pi^2)^{2/3}\rho^{5/3}]$, and α . In the bulk ($z \rightarrow -\infty$), both s and q are small, while $\alpha \rightarrow 1$ (showing that the Thomas-Fermi theory becomes exact). In the vacuum, all semilocal ingredients diverge (as in the case of the jellium surface).

In the limit $z \rightarrow \infty$, the Airy-gas electron density and kinetic-energy density are

$$\begin{aligned} \rho(z \rightarrow \infty) &\rightarrow \frac{1}{32} \frac{e^{-4/3 z^{3/2}}}{\pi^2 z^{3/2}} - \frac{35}{768} \frac{e^{-4/3 z^{3/2}}}{\pi^2 z^3} + \dots \\ \tau(z \rightarrow \infty) &\rightarrow \frac{1}{64} \frac{e^{-4/3 z^{3/2}}}{\sqrt{z}\pi^2} + \frac{13}{1536} \frac{e^{-4/3 z^{3/2}}}{\pi^2 z^2} + \dots \end{aligned} \quad (12)$$

The SA-TPSS XC functional gives the following analytical expressions:

$$\begin{aligned} \epsilon_{xc}^{SA-TPSS}(z \rightarrow \infty) &\rightarrow -\sqrt{3}/(8z) \approx -0.217/z, \\ v_{xc}^{SA-TPSS}(z \rightarrow \infty) &\rightarrow -3\sqrt{3}/(16z) \approx -0.325/z \end{aligned} \quad (13)$$

This result is interesting, since it suggests that, for the Airy gas, both ϵ_{xc} and v_{xc} decay as $-1/z$, as in the case of the jellium surface. Furthermore, because the coefficients (0.217 and 0.325) are close to, but smaller than, the ones for the jellium surface (0.25 and 0.375), we can conclude that at a metal surface the main contribution to the asymptotics comes from the region near the surface, where the effective potential is linear and well described by the Airy-gas model. We note that such a result cannot be obtained without the proper inclusion of exact surface conditions into the functional. This is shown in Fig. 4 where we plot, for several functionals, $z\epsilon_{xc}(z)$ (upper panel) and $zv_{xc}(z)$ (lower panel), versus the scaled distance z , in the vacuum region of the Airy gas. The TPSS functional shows a rather unphysical exponential decay for both ϵ_{xc} and v_{xc} . On the other hand, the AM05 functional⁵², whose energy density is fitted to the Airy gas, is close to our SA-TPSS functional for ϵ_{xc} but displays

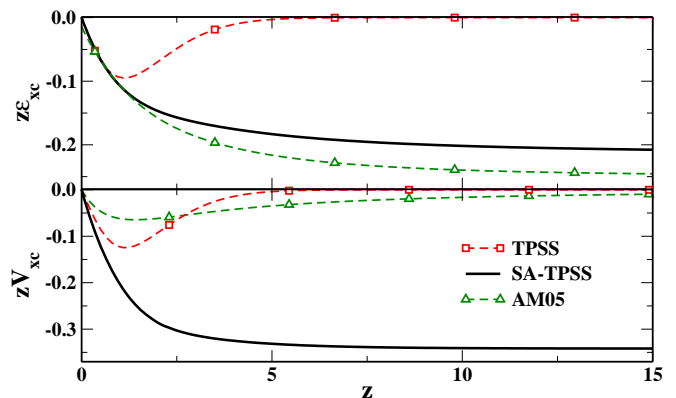


FIG. 4: The Airy-gas $z\epsilon_{xc}(z)$ (upper panel) and $zv_{xc}(z)$ (lower panel), as a function of the scaled distance z .

a decay that is too fast for v_{xc} . This latter feature represents a manifestation of the impossibility, at the GGA level, to describe correctly both ϵ_{xc} and v_{xc} , which can only be overcome at the meta-GGA level³⁸.

The exchange-only asymptotic behaviors (ϵ_x and v_x) at metal surfaces, are depending on the bulk and surface parameters (k_F and W)²⁷⁻²⁹, and thus they are created by bulk- and surface-electrons. When correlation is included, screening effects dump the bulk contribution, such that the asymptotic properties of ϵ_{xc} and v_{xc} are mainly created by a density-independent XC effect of the surface region, as proved by the SA-TPSS result for the Airy gas. Thus, the Airy gas model system can be efficiently used in modelling various phenomena outside metal surfaces, even being an alternative to the ad-hoc LDA XC potential modifications^{18,19}.

V. CONCLUSIONS

In conclusion, we have derived an exact meta-GGA condition for the correct image-like surface asymptotics of the XC energy per particle ϵ_{xc} and the KS XC potential v_{xc} . Our formula [Eq. (5)] depends only on the semilocal ingredient α and takes advantage of the non-locality of the kinetic energy density beyond the von Weizsäcker term³⁸. The existence of this exact condition represents an important contribution in the framework of DFT, as it shows that surface asymptotics can be described by semilocal meta-GGA functionals. On the contrary, no GGA can be constructed that is able to describe correctly the asymptotics of both ϵ_{xc} and v_{xc} . In fact, there is, to our knowledge, no GGA functional that yields a realistic KS XC potential at metal surfaces.

We have demonstrated that our exact condition can be easily implemented in any meta-GGA functional, keeping its original accuracy for standard ground-state properties and providing, at the same time, a correct description of the surface asymptotics. We have constructed the SA-TPSS functional, which we have shown to perform as the

TPSS for covalent chemistry and to improve over it for non-covalent interactions and surface-related problems. This new functional can thus be a promising tool for the investigation of surface-sensitive electronic-structure calculations, such as molecule/molecular complex-surface, cluster-surface, and surface-surface interactions.

We thank TURBOMOLE GmbH for providing the TURBOMOLE program package.

APPENDIX A

In case of semi-infinite jellium surfaces, the one-particle eigenfunctions $\phi_{k_z}(z)$ have a continuous energy spectrum $\epsilon_{k_z} = V_{KS}(\infty) + k_z^2/2$, and are solutions of the one-dimensional KS equation

$$\left(-\frac{\partial^2}{2\partial z^2} + V_{KS}(z) - \epsilon_{k_z}\right)\phi_{k_z}(z) = 0. \quad (\text{A-1})$$

Here $V_{KS}(z) = V_H(z) + V_{xc}(z)$ is the sum of the total classical electrostatic potential (which incorporates the positive background), and the XC potential.

In case of the Airy gas, the effective potential has the linear form

$$v_{eff}(Z) = \begin{cases} -FZ & \text{when } -\infty < Z < L \\ +\infty & \text{when } Z \geq L, \end{cases} \quad (\text{A-2})$$

with $F > 0$ being the slope of the effective potential⁵¹. Thus, the one-particle normalized eigenfunctions $\phi_j(Z)$

satisfy the one-dimensional equation

$$\begin{aligned} \left(-\frac{\partial^2}{2\partial Z^2} - FZ - \epsilon_j\right)\phi_j(Z) &= 0, \\ \phi_j(\infty) &= \phi_j(L) = 0, \end{aligned} \quad (\text{A-3})$$

being proportional to the Airy function. Here Z is the distance perpendicular to the surface. It is convenient to consider the scaled distance $z = Z(2F)^{1/351}$, as used in the Section IV.

APPENDIX B

The electron density and kinetic energy density of a jellium surface are

$$\rho(z) = \frac{1}{4\pi^2} \int_{-k_F}^{k_F} dk_z (k_F^2 - k_z^2) |\phi_{k_z}(z)|^2, \quad (\text{B-1})$$

$$\begin{aligned} \tau(z) &= \int_{-k_F}^{k_F} dk_z \left[\frac{1}{8\pi^2} \left| \frac{\partial \phi_{k_z}(z)}{\partial z} \right|^2 (k_F^2 - k_z^2) + \right. \\ &\quad \left. \frac{1}{16\pi^2} |\phi_{k_z}(z)|^2 (k_F^2 - k_z^2)^2 \right], \end{aligned} \quad (\text{B-2})$$

with k_F being the magnitude of the bulk Fermi wave-vector.

Using Eqs. (3) and (4) we obtain, when $z \rightarrow \infty$, the following expressions

$$\rho \rightarrow \left(\frac{1}{4} \frac{N^2 W}{k_F \pi^2 z^2} - \frac{1}{8} \frac{N^2 \sqrt{2} W^{3/2}}{k_F^3 z^3 \pi^2} \right) e^{-2z\sqrt{2W}} z^{2\alpha_{KS}} \quad (\text{B-3})$$

$$\begin{aligned} \tau \rightarrow & \frac{1}{4} \frac{N^2 W^2}{k_F \pi^2 z^2 e^{2z\sqrt{2W}} z^{-2\alpha_{KS}}} + \frac{1}{32} \frac{\left(-8 k_F^4 \sqrt{W} \alpha_{KS} - 4 k_F^2 W^{3/2} + 12 k_F^4 \sqrt{W} \right) N^2 W \sqrt{2}}{k_F^5 \pi^2 z^3 e^{2z\sqrt{2W}} z^{-2\alpha_{KS}}} + \\ & \frac{1}{32} \frac{\left(-12 k_F^2 W \sqrt{2} + 3 \sqrt{2} k_F^4 + 4 k_F^2 W \sqrt{2} \alpha_{KS} - 4 \sqrt{2} k_F^4 \alpha_{KS} + 2 \sqrt{2} k_F^4 \alpha_{KS}^2 \right) N^2 W \sqrt{2}}{k_F^5 \pi^2 z^4 e^{2z\sqrt{2W}} z^{-2\alpha_{KS}}} + \\ & \frac{1}{32} \frac{\left(6 k_F^2 \sqrt{W} \alpha_{KS} + 6 W^{3/2} - 2 k_F^2 \sqrt{W} \alpha_{KS}^2 - 6 k_F^2 \sqrt{W} \right) N^2 W \sqrt{2}}{k_F^5 \pi^2 z^5 e^{2z\sqrt{2W}} z^{-2\alpha_{KS}}}. \end{aligned} \quad (\text{B-4})$$

Then,

$$\alpha \rightarrow - \frac{\left(-60 \sqrt[3]{3} \sqrt[3]{2} k_F^2 z \sqrt{W} + 40 \sqrt[3]{3} 2^{2/3} W - 15 \sqrt[3]{3} 2^{2/3} k_F^2 \right) e^{4/3 z \sqrt{2W}} z^{-4/3 \alpha_{KS} - 2/3} 2^{2/3}}{54 W^{2/3} N^{4/3} k_F^{4/3}}, \quad (\text{B-5})$$

and

$$F_{xc} \rightarrow \frac{4}{9\eta} \frac{\left(\pi 2^{2/3} 3^{2/3} \sqrt[3]{k_F} + 9 O(z^{-4/3}) N^{2/3} \sqrt[3]{W} \sqrt[3]{z} \right) e^{2/3 z \sqrt{2W}} z^{-2/3 \alpha_{KS} - 1/3}}{N^{2/3} \sqrt[3]{W}}, \quad (\text{B-6})$$

where N is a normalization constant, W is the work function, and k_F is the bulk Fermi wave-vector. Here

$F_{xc} = \epsilon_{xc}^{MGGA}/\epsilon_{xc}^{LDA}$ is the enhancement factor corresponding to the energy density of Eq. (5).

-
- ¹ N. Garcia, B. Reihl, K. H. Frank, and A. R. Williams, Phys. Rev. Lett. **54**, 591 (1985), URL <http://link.aps.org/doi/10.1103/PhysRevLett.54.591>.
- ² S. Datta, *Quantum transport: atom to transistor* (Cambridge University Press, 2005).
- ³ J. Rundgren and G. Malmström, Phys. Rev. Lett. **38**, 836 (1977).
- ⁴ G. Binnig, K. H. Frank, H. Fuchs, N. Garcia, B. Reihl, H. Rohrer, F. Salvan, and A. R. Williams, Phys. Rev. Lett. **55**, 991 (1985).
- ⁵ J. Pitarke, F. Flores, and P. Echenique, Surf. Sci. **234**, 1 (1990), ISSN 0039-6028.
- ⁶ C. B. Harris, N.-H. Ge, R. L. L. Jr., J. D. McNeill, and C. M. Wong, Ann. Rev. Phys. Chem. **48**, 711 (1997).
- ⁷ T. Fauster and W. Steinmann, in *Electromagnetic Waves: Recent Development in Research, Vol. 2*, edited by P. Halevi (Elsevier, Amsterdam, 1995), p. 350.
- ⁸ N. Lang and W. Kohn, Phys. Rev. B **7**, 3541 (1973).
- ⁹ W. Kohn, Rev. Mod. Phys. **71**, 1253 (1999).
- ¹⁰ W. Kohn and L. J. Sham, Phys. Rev. **140**, A1133 (1965).
- ¹¹ O. Gunnarsson, M. Jonson, and B. I. Lundqvist, Phys. Rev. B **20**, 3136 (1979), URL <http://link.aps.org/doi/10.1103/PhysRevB.20.3136>.
- ¹² A. G. Eguiluz and W. Hanke, Phys. Rev. B **39**, 10433 (1989).
- ¹³ A. G. Eguiluz, M. Heinrichsmeier, A. Fleszar, and W. Hanke, Phys. Rev. Lett. **68**, 1359 (1992).
- ¹⁴ I. D. White, R. W. Godby, M. M. Rieger, and R. J. Needs, Phys. Rev. Lett. **80**, 4265 (1998).
- ¹⁵ Z. Qian and V. Sahni, Int. J. Quantum Chem. **104**, 929 (2005).
- ¹⁶ J.-T. Hoefft, M. Kittel, M. Polcik, S. Bao, R. L. Toomes, J.-H. Kang, D. P. Woodruff, M. Pascal, and C. L. A. Lamont, Phys. Rev. Lett. **87**, 086101 (2001).
- ¹⁷ A. D. Becke, Phys. Rev. A **38**, 3098 (1988).
- ¹⁸ P. A. Serena, J. M. Soler, and N. García, Phys. Rev. B **34**, 6767 (1986), URL <http://link.aps.org/doi/10.1103/PhysRevB.34.6767>.
- ¹⁹ E. Chulkov, V. Silkin, and P. Echenique, Surface Science **437**, 330 (1999), ISSN 0039-6028.
- ²⁰ O. Gunnarsson and R. O. Jones, Physica Scripta **21**, 394 (1980), URL <http://iopscience.iop.org/1402-4896/21/3-4/027>.
- ²¹ S. Ossicini, C. M. Bertoni, and P. Gies, Europhy. Lett. **1**, 661 (1986).
- ²² P. García-González, J. E. Alvarellos, E. Chacón, and P. Tarazona, Phys. Rev. B **62**, 16063 (2000).
- ²³ J. Harris and A. Griffin, Phys. Rev. B **11**, 3669 (1975).
- ²⁴ D. C. Langreth and J. P. Perdew, Phys. Rev. B **15**, 2884 (1977).
- ²⁵ O. Gunnarsson and B. I. Lundqvist, Phys. Rev. B **13**, 4274 (1976).
- ²⁶ L. A. Constantin and J. M. Pitarke, Phys. Rev. B **83**, 075116 (2011).
- ²⁷ C. M. Horowitz, L. A. Constantin, C. R. Proetto, and J. M. Pitarke, Phys. Rev. B **80**, 235101 (2009).
- ²⁸ Z. Qian, Phys. Rev. B **85**, 115124 (2012).
- ²⁹ C. M. Horowitz, C. R. Proetto, and J. M. Pitarke, Phys. Rev. B **81**, 121106 (2010).
- ³⁰ C. M. Horowitz, C. R. Proetto, and S. Rigamonti, Phys. Rev. Lett. **97**, 026802 (2006), URL <http://link.aps.org/doi/10.1103/PhysRevLett.97.026802>.
- ³¹ C. M. Horowitz, C. R. Proetto, and J. M. Pitarke, Phys. Rev. B **78**, 085126 (2008), URL <http://link.aps.org/doi/10.1103/PhysRevB.78.085126>.
- ³² L.-H. Ye, Phys. Rev. B **92**, 115132 (2015).
- ³³ E. Engel, J. Chem. Phys. **140**, 18A505 (2014).
- ³⁴ E. Engel, Phys. Rev. B **89**, 245105 (2014).
- ³⁵ E. Engel, J. Chevary, L. Macdonald, and S. Vosko, Z. Phys. D **23**, 7 (1992), ISSN 0178-7683.
- ³⁶ R. van Leeuwen and E. J. Baerends, Phys. Rev. A **49**, 2421 (1994).
- ³⁷ R. Armiento and S. Kümmel, Phys. Rev. Lett. **111**, 036402 (2013).
- ³⁸ F. Della Sala, E. Fabiano, and L. A. Constantin, Phys. Rev. B **91**, 035126 (2015).
- ³⁹ N. D. Lang and W. Kohn, Phys. Rev. B **1**, 4555 (1970).
- ⁴⁰ N. Lang and W. Kohn, Phys. Rev. B **3**, 1215 (1971).
- ⁴¹ B. Silvi and A. Savin, Nature **371**, 683 (1994).
- ⁴² A. V. Arbuznikov, M. Kaupp, V. G. Malkin, R. Reviakine, and O. L. Malkina, Phys. Chem. Chem. Phys. **4**, 5467 (2002).
- ⁴³ J. Tao, J. P. Perdew, V. N. Staroverov, and G. E. Scuseria, Phys. Rev. Lett. **91**, 146401 (2003).
- ⁴⁴ L. A. Constantin, A. Terentjevs, F. Della Sala, and E. Fabiano, Phys. Rev. B **91**, 041120 (2015).
- ⁴⁵ D. V. Feinblum, J. Kenison, and K. Burke, J. Chem. Phys. **141**, 241105 (2014).
- ⁴⁶ B. Wood, N. D. M. Hine, W. M. C. Foulkes, and P. García-González, Phys. Rev. B **76**, 035403 (2007).
- ⁴⁷ J. P. Perdew and Y. Wang, Phys. Rev. B **45**, 13244 (1992).
- ⁴⁸ J. P. Perdew, K. Burke, and M. Ernzerhof, Phys. Rev. Lett. **77**, 3865 (1996).
- ⁴⁹ L. A. Constantin, E. Fabiano, and F. D. Sala, J. Chem. Theory Comput. **9**, 2256 (2013).
- ⁵⁰ E. Fabiano, L. A. Constantin, and F. Della Sala, Int. J. Quantum Chem. **113**, 673 (2013), ISSN 1097-461X, URL <http://dx.doi.org/10.1002/qua.24042>.
- ⁵¹ W. Kohn and A. E. Mattsson, Phys. Rev. Lett. **81**, 3487 (1998).
- ⁵² R. Armiento and A. E. Mattsson, Phys. Rev. B **72**, 085108 (2005).
- ⁵³ L. Vitos, B. Johansson, J. Kollár, and H. L. Skriver, Phys. Rev. A **61**, 052511 (2000).
- ⁵⁴ L. A. Constantin and A. Ruzsinszky, Phys. Rev. B **79**, 115117 (2009).
- ⁵⁵ L. Vitos, B. Johansson, J. Kollár, and H. L. Skriver, Phys. Rev. B **62**, 10046 (2000).